

Projectile fragmentation of silicon ions at 490 A MeV

F. Flesch¹, G. Iancu¹, W. Heinrich¹, and H. Yasuda²

¹Department of Physics, University of Siegen, 57068 Siegen, Germany

²National Institute of Radiological Sciences (NIRS), Chiba-shi, Inage-ku, Anagawa 4-9-1, Chiba 263, Japan

Abstract. We have used stacks containing CR-39 nuclear track detectors and different target materials C, CH₂, Al, Cu, Ag and Pb to measure charge changing and elemental fragmentation cross sections of heavy ion projectiles. Due to the detection threshold of the CR-39 material, we observe fragments with charge numbers $Z \geq 6$. For experiments exposed to Si ions at 490 A MeV at the HIMAC (Chiba, Japan) we presented first results for the carbon target at the last ICRC. The analysis of this experiment has been completed. In this paper we present our final results for all target materials and compare them to other experimental data and to model predictions.

1. Introduction

Fragmentation cross sections are essential input parameters for propagation calculations which describe the effect of shielding against cosmic ray heavy nuclei by the walls of space craft or planetary habitat. Cross sections for the breakup of different elements are needed for different types of target material and for a wide range of energy. For this purpose we have extended our studies of projectile fragmentation.

For this experiment ²⁸Si ions at 490 A MeV were accelerated against different target material. The detector used was CR-39 (C₁₂H₁₈O₇).

2. Experimental Method

The use of CR-39 detector enables us to determine the trajectories and the charges of the projectile ions and their fragments. The experimental setup consists of stacks of 5 detector foils upstream and 12 detector foils downstream each target traversed perpendicularly by the beam ions. The thickness of a typical detector foil is about 640 μm. The targets have been chosen to have a thickness of about 10% of the interaction mean free path of the beam particles. This value was found to be a good compromise to maximize the number of projectile fragments produced inside the target without generating too many re-interactions of these fragments inside the target.

We have exposed a set of 9 stacks containing the following targets CH₂, C, Al, Cu, Ag, and Pb at the HIMAC in Chiba, Japan. The energy of the incident ²⁸Si ion beam was 490 A MeV. The corresponding energy in the middle of each target vary from 467 for H and C to 430 for Pb. For each stack an area of 10x10cm² was irradiated with a mean beam density of 900 particles/cm². The ionization of the particles causes latent tracks along their trajectories. After etching of the detector foils in 6 N NaOH at 60°C for 50 hours cone shaped etch pits were developed on the detector surfaces along the latent tracks. Their size is related to the energy loss of the ions.

We have used a completely automatic measuring system (Trakowski et al., 1984; Heinrich et al., 1995 and references therein). Parameters such as the track positions on the detector foils, track area, shape of the etch figures and other quantities were extracted from the video picture. Fig. 1. shows a typical image seen by the measuring system.

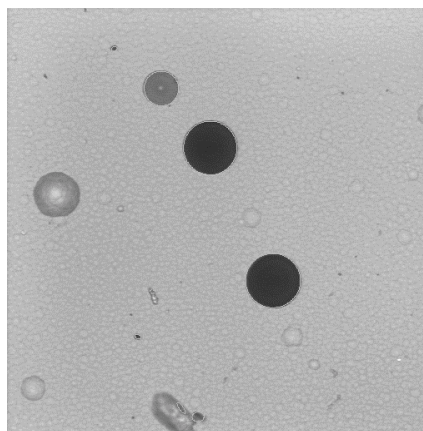


Fig. 1 Typical video image

Since the projectile fragments due to their lower charge have a lower LET as the projectile particles their etch-pit circles are flatter, so that their etch figures show higher brightness value. Surface structures enlarged by the etch process as well as tracks of stopping target fragments and alpha particles from Radon decay are expected to be seen in the detector. The picture (Fig.1) shows the etch-pit circles of two primary particles (large dark circular objects), a

projectile fragment (smaller gray circular object) and some surface structures (non circular objects and a circular object with a large bright center). We measure the central brightness of all objects to separate the tracks of beam particles and beam fragments which are of interest for us. In Fig. 2 we have plotted the track areas of all measured objects on a single detector foil side versus their measured value of central brightness.

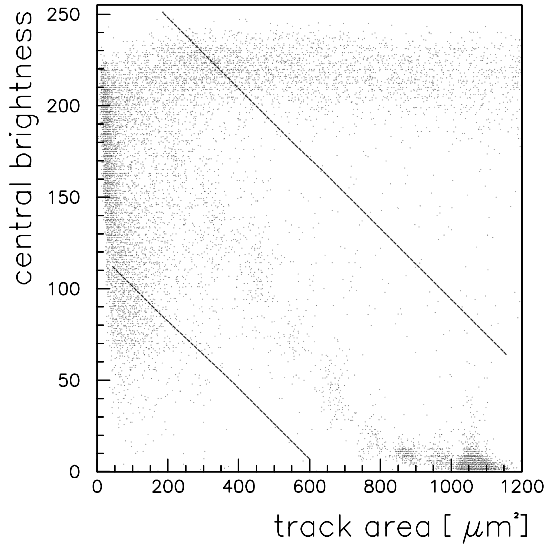


Fig. 2 Data reduction by cross plots of the track areas versus the central brightness values of the measured objects.

We can identify in this figure the beam particles and their fragments as groups of measured objects at values of smaller central brightness (<50) and larger track areas ($>700 \mu\text{m}^2$). The central brightness values of the fragments increase with decreasing track areas, as expected. Clusters of objects with track areas below $700 \mu\text{m}^2$ and increasing values of central brightness can be seen. A large part of the measured surface structures can well be separated from the etch-pit circles of the projectiles and their fragments, by using cuts in these plots indicated by the dashed lines. After the data reduction by excluding a part of the surface structures, individual particle trajectories were reconstructed through all foil sides in the front and in the back stack. For this purpose we used specially developed software capable of tracing particle trajectories through successive detector foils. After the reconstruction of the particle trajectories the surface structures are completely excluded and charge peaks can clearly be identified in plots of the track areas of all traced objects of a single detector foil side. The charge calibration of the detectors is based on these charge peaks on each foil side. For detail see Flesch et al., (1999). By using multiple track measurements on successive foil sides the charge resolution can be improved significantly (Flesch et al., 1999). This way we get charge resolutions between 0.1e and 0.12e for the fragments

charge numbers $Z_F=6-13$. Using these mean charge distributions on the last foil side in the front and in the first foil side in the back stack, the total and elemental charge changing cross sections can be computed by using the propagation methods described by Brechtmann et al., (1988).

3. Results and Discussion

Table 1. Measured total and elemental charge changing fragmentation cross section.

The measured total and elemental charge changing cross sections are listed in Tab. 1, the given errors including the statistical and the systematical ones.

	Total and elemental fragmentation cross sections for ^{28}Si in [mb]		
	H target	C target	Al target
E_{Target} [A MeV]	467	467	453
σ_{tot}	367.6 ± 16.7	1136.4 ± 12.8	1637.7 ± 23.0
$\sigma(Z_F=13)$	65.0 ± 6.4	125.3 ± 4.7	162.5 ± 8.0
$\sigma(Z_F=12)$	78.6 ± 6.9	129.5 ± 4.8	163.6 ± 8.0
$\sigma(Z_F=11)$	40.9 ± 4.8	66.7 ± 3.4	93.6 ± 6.0
$\sigma(Z_F=10)$	35.1 ± 4.8	77.1 ± 3.5	97.0 ± 6.0
$\sigma(Z_F=9)$	12.2 ± 3.1	37.8 ± 2.4	50.1 ± 4.0
$\sigma(Z_F=8)$	24.7 ± 4.4	79.4 ± 3.5	102.4 ± 6.0
$\sigma(Z_F=7)$	15.7 ± 3.6	61.5 ± 3.1	78.7 ± 5.0
$\sigma(Z_F=6)$	33.2 ± 4.7	84.6 ± 3.6	112.4 ± 6.0
	Cu target	Ag target	Pb target
E_{Target} [A MeV]	442	436	430
σ_{tot}	2200.8 ± 29.2	2871.8 ± 47.8	3751.3 ± 63.3
$\sigma(Z_F=13)$	192.9 ± 9.9	233.9 ± 15.6	362.3 ± 24.0
$\sigma(Z_F=12)$	198.2 ± 9.7	241.1 ± 15.4	342.9 ± 21.9
$\sigma(Z_F=11)$	100.3 ± 6.7	128.5 ± 11.2	132.1 ± 13.6
$\sigma(Z_F=10)$	95.2 ± 6.5	141.5 ± 11.7	163.1 ± 15.4
$\sigma(Z_F=9)$	61.1 ± 5.2	61.7 ± 7.8	70.4 ± 9.4
$\sigma(Z_F=8)$	120.6 ± 7.3	151.9 ± 11.9	171.1 ± 14.9
$\sigma(Z_F=7)$	90.3 ± 6.2	105.6 ± 10.0	123.8 ± 12.4
$\sigma(Z_F=6)$	143.7 ± 8.0	177.6 ± 13.1	190.1 ± 15.3

The energy E_{Target} in Tab. 1 means the kinetic energy in the middle of the target. The cross sections for H target were determined from the measured data for CH_2 and C target. In Fig.3., we have compared the total charge changing cross sections for H and C target to the results from our earlier experiments at 1 and 2 A GeV (Hirzebruch, 1993) and 14.5 A GeV (Brechtmann et al., 1988). Furthermore we have compared our results to the measurements of Webber et al. (1990). Additionally we have plotted the predictions of the models from Kox et al. (1987) and Letaw et al. (1983). Both models predict total

reaction cross sections. To compare these models with the measured charge changing cross sections the contribution of the non-charge changing neutron loss was calculated from the semi-empirical model from Silberberg et al. (1998) and subtracted from the predictions. All measured cross sections are in a good agreement within their errors. It looks like that the cross sections are slowly decreasing with decreasing energy below a projectile energy of 1 A GeV as predicted from the models. For the C target data the cross sections measured by Webber tend to exceed our data points for all measured energies. For the heavier target data our measured total cross sections in the energy range between 450 A MeV and 14.5 A GeV show only a significant energy dependence for the heavier targets like Ag and Pb. This increase of the cross sections with increasing projectile energy is caused by the contributions by electromagnetic dissociation with increasing energy. In Fig. 4 we have plotted our elemental fragmentation cross section values for the different beam energies and the targets C and Al. For the C target data the cross sections for fragment $Z_F=10, 11, 12, 13$ show a systematic increase of the cross sections with decreasing energy below 2 A GeV. For fragment charge numbers 7, 8, 9 the cross sections show a more constant behavior. Similar energy dependence can be observed for the Al target data.

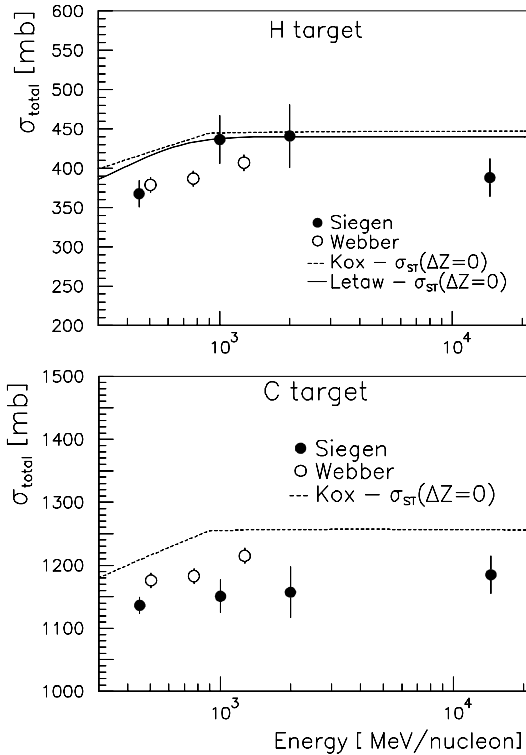


Fig. 3 Comparison of our measured total charge changing cross sections (including Hirzebruch et al. for 1 and 2 A GeV, 1993 and Brechtmann et al. for 14.5 A GeV, 1988) to the results measured by Webber et al. (1990) and to model predictions.

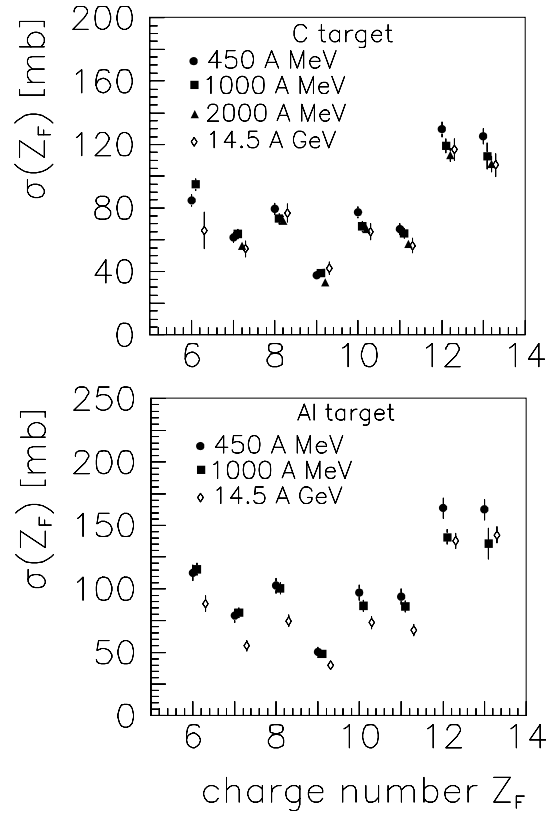


Fig. 4 Comparison of our measured elemental fragmentation cross sections for C and Al target at different projectile energies.

Acknowledgments. Our experiment was funded by the DLR under contract number 50WB9902. We are grateful to the staff of the Chiba HIMAC for providing us with heavy ion beams.

References

- Brechtmann, C., Heinrich, W., Measurements of elemental fragmentation cross section for relativistic heavy ions using CR-39 plastic nuclear track detectors. Nucl. Instr. and Meth. B29, 675-679, 1988.
- Flesch, F., Hirzebruch, S.E., Hüntrup, G., Röcher, H., Streibel, T., Winkel, E., Heinrich, W., Fragmentation cross section measurements of iron projectiles using CR-39 plastic nuclear track detectors. Radiat. Meas., 31, 533-536, 1999.
- Heinrich, W., Becker, E., Dreute, J., Hirzebruch, S.E., Hüntrup, G., Kurth, M., Röcher, H., Schmitz, M., Streibel, T., Winkel, E., High energy heavy ion interactions studied with SSNTDs., Radiation Measurements 25, 203-218, 1995.
- Kox, S., Gamp, A., Perrin, C., Arvieux, J., Bertholet, R., Bruandet, J.F., Buenerd, M., Cherkaoui, R., Cole, A.J., El-Masri, Y., Longequeue, N., Menet, J., Merchez, F., Viano, J.B., Trends of total reaction cross sections for heavy ion collisions in the intermediate energy range., Phys. Rev C35, 1678-1690, 1987.
- Letaw, J. R., Silberberg, R., Tsao, C. H., Proton-nucleus total inelastic cross sections: An empirical formula for $E > 10$ MeV., Astrophys. J. Suppl. 51, 271-276, 1984.

- Silberberg, R., Tsao, C. H., Barghouty, A.F., Updated partial cross sections of proton-nucleus reactions., *Astrophys. J.* 50 501, 911-919, 1998.
- Trakowski, W., Schöfer, B., Dreute, J., Sonntag, S., Brechtmann, C., An automatic measuring system for particle track detectors., *Nucl. Instr. and Meth.* 255, 92-100, 1984.
- Webber, W. R., Kish, J. C., Schrier, D. A., Individual charge changing fragmentation cross sections of relativistic nuclei in hydrogen, helium, and carbon targets., *Phys. Rev. C* 41, 533-546, 1990.
- Hirzebruch, S.E., Projektilfragmentation relativistischer ^{16}O , ^{19}F , ^{27}Al , ^{28}Si und ^{56}Fe Schwerionen, Thesis, University of Siegen, 1993